Surface analysis of palladium boride liquid metal ion beam deposition on silicon single-crystal solid surface

R. H. Higuchi-Rusli, J. C. Corelli, A. J. Steckl, and H.-S. Jin
Center for Integrated Electronics, Rensselaer Polytechnic Institute, Troy, New York 12181

(Received 23 September 1986; accepted 29 December 1986)

Surface analysis of a palladium boride liquid metal ion beam deposition on a silicon single-crystal (100) solid surface was analyzed by optical microscopy, Auger electron spectroscopy, and Rutherford backscattering spectroscopy. The beam composition prior to the deposition on silicon was analyzed with a quadrupole mass spectrometer. Droplet formation was observed experimentally from a 10-μm emitter tip radius which can be estimated from calculation to be due to higher mass flow rate associated with a larger emitting tip radius. Auger electron spectroscopy results show that the main element contaminants (Fe, Ni, Cr, and Re) come mostly from extractor material (Fe, Ni, and Cr) sputtering, and emitter tip erosion. Rutherford backscattering analysis of beam deposit from a 10-μm emitter tip radius on silicon surface shows no change in stoichiometry between the deposit and alloy source despite droplet formation on silicon surface.

I. INTRODUCTION

Liquid metal ion sources (LMIS's) attract considerable interest because of their use in microelectronics fabrication. In the focused ion beam system (FIB), LMIS has emerged as a primary source for submicron level fabrication of integrated circuit (IC) devices.[1–3] Droplet emission from LMIS was first thought to be a problem inherent to capillary emitter-type LMIS. The calculated results presented in this paper show that the mass flow rate to the emitter tip is governed by the emitter tip size and the total mass fraction emitted in the form of charged droplets is related to the flow resistance of liquid metal in the tip region.[4,5] The droplet phenomena has been indirectly verified in a number of experiments such as by microscopic observation of droplets on an operating liquid metal tip,[6] and by observation of droplet-like features on LMIS-bombarded surfaces.[7,8] The mixed beam or spray of ions and droplets frozen upon impact on any substrate can be used to build up a coating by the technique known as field emission deposition (FED).[7] It has also recently been reported that a beam of charged droplets can be focused and steered electrically.[9] Therefore, deposition by liquid metal ion source has a potential application for direct writing of patterns such as conducting pathways in hybrid microcircuits.[9]

Liquid metal ion sources fabricated from metallic glass material such as PdB binary alloy have potential application for surface wear resistance due to higher adherence of films produced by FED. A fracture strength in excess of 10^8 N m^{-2} has been reported with potential benefit in thermal compression bonding applications.[7] For both microelectronics and microcoating applications, stable beam composition must be maintained by minimizing contaminants which result from extractor sputtering and chemical interaction between emitter and alloy source. In this paper, particular attention is given on the composition of the beam deposit and the causes of droplet formation.

II. EXPERIMENT

Figure 1 shows the experimental setup with a silicon single-crystal solid substrate placed on a rectractable sample holder. The dual carbon filament LMIS used as the deposition source is located above the sample. Beam composition was analyzed by retracting the sample holder out of the beam path and allowing the beam to pass through the quadrupole mass spectrometer. The distance from the emitter to the sample is 1 cm to insure maximum beam capture on the silicon surface. The whole setup consists of a retractable sample holder, filament, and ionizing chamber for residual gas analysis, and a series of lenses to focus the ion beam into the quadrupole mass spectrometer. The quadrupole mass spectrometer was calibrated with a gallium LMIS before this

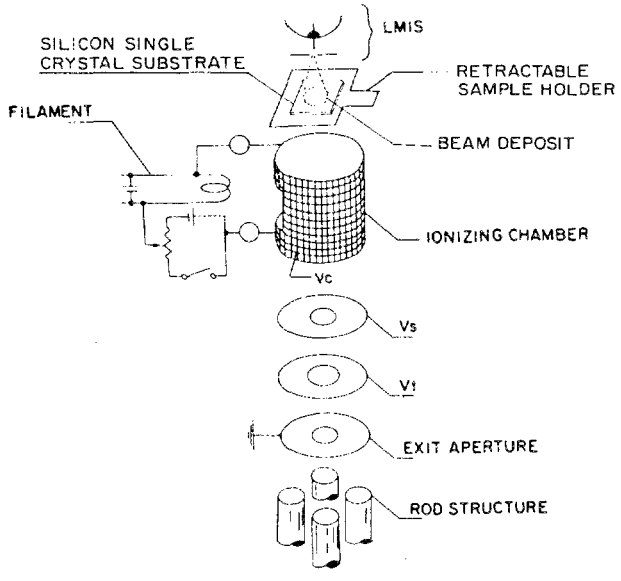

FIG. 1. Schematic setup of liquid metal ion source deposition on silicon substrate.

 0734-2101/87/041362-05$01.00

experiment to insure accuracy of the mass spectrometer response for the PdB source. The dual carbon filament LMIS built and developed at the CIE–RPI laboratory was used throughout this experiment.[10] Two different emitter radii (2.5 and 10 μm) made of Re were prepared by mechanical grinding, followed by electrochemical etch (2 min) with 5N NaOH. Input heater power of 80 W was required to melt the alloy and maintain the liquid flow to the emitter tip. Applied extraction voltages of 6.5 and 7.0 kV were used with 2.5- and 10-μm emitter, respectively. The length of deposition time was 3 h for each sample. Consistency of beam composition was maintained by retracting the sample holder out of the beam path periodically in every 1-h run, so that the peak height of the beam elements could be monitored closely by the mass spectrometer. Liquid metal ion source heater power is used to maintain constant peak height (beam current) throughout the experiment.

III. RESULT AND DISCUSSION

A typical mass spectrum of a palladium boride LMIS with 2.5-μm radius emitter tip is shown in Fig. 2. The beam composition with 2.5- and 10-μm radius emitter tip is tabulated in Tables I and II. The applied extractor voltage was 6.5 and 7.0 kV for the 2.5- and 10-μm in radius tip, respectively. The percent abundance of boron species produced with 2.5-μm emitter is almost twice as high as the boron species produced from 10-μm emitter. The average $^{11}B^+$ current recorded (with no attempt to focus the beam) was 0.41 and 0.16 μA for 2.5- and 10-μm emitter tip radius, respectively. This result represents 12% and 7.2% of the total current recorded by quadrupole mass spectrometry (QMS). From the tabulated elements in Tables I and II, $(B/Pd)_{beam}$ are 12.3% and 10.9% which is less than $(B/Pd)_{alloy}$. Figures 3 and 4 show $^{11}B^+$ current–voltage and total extractor current–voltage characteristics of $Pd_{73}B_{27}$ alloy with 2.5- and 10-μm emitter tip radius, respectively. For both emitters the difference is more significant at higher applied voltage where the $^{11}B^+$ current tends to saturate. An interesting result shows that despite the higher total current yield from the 2.5-μm emitter tip, the yield of singly ionized palladium and its molecules PdB^+ is smaller compared with 10-μm emitter tip and is due to the small size of the tip apex which reduces the flow rate to the emitter tip.

Figure 5 shows a plot of mass flow rate versus emitter radius calculated from the Poisseuille equation and the force acting along the cone axis.[11]

For small emitter tip (2.5-μm radius) the liquid metal flow rate is small due to the shorter time required to replen-

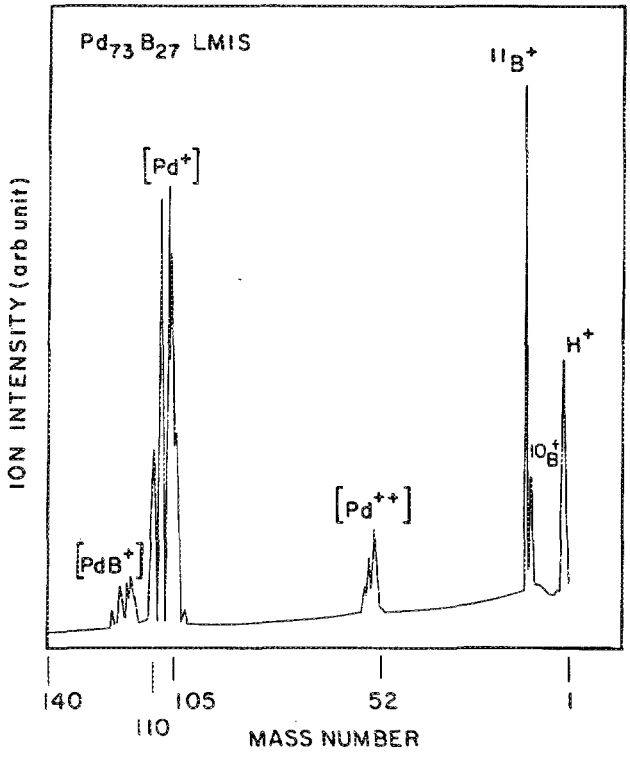

FIG. 2. A typical palladium boride mass spectrum from LMIS.

TABLE I. % abundance of various elements in beam at 3.38 μA for Pd–B alloy on Re emitter (tip radius: 2.5 μm).

Elements	Current (A)	% abundance
$^{11}B^+$	4.1×10^{-7}	12.13
$^{10}B^+$	2.0×10^{-7}	5.91
$^{104}Pd^{++}$	1.0×10^{-7}	2.96
$^{106}Pd^{++}$	2.3×10^{-7}	6.80
$^{105}Pd^{++}$	9×10^{-8}	2.66
$^{110}Pd^{++}$	3.0×10^{-8}	0.89
$^{102}Pd^+$	4.0×10^{-8}	1.18
$^{104}Pd^+$	4.6×10^{-8}	1.36
$^{105}Pd^+$	4.5×10^{-7}	13.31
$^{106}Pd^+$	6.2×10^{-7}	18.34
$^{108}Pd^+$	6.0×10^{-7}	17.75
$^{110}Pd^+$	3.0×10^{-7}	8.87
$^{104}Pd^{++}B^+$	8.0×10^{-8}	2.37
$^{106}Pd^{11}B^+$	7.0×10^{-8}	2.07
$^{108}Pd^{11}B^+$	6.0×10^{-8}	1.77
$^{110}Pd^{11}B^+$	5.0×10^{-8}	1.48

TABLE II. % abundance of various elements in beam at 2.23 μA for Pd–B alloy on Re emitter (tip radius: 10 μm).

Elements	Current (A)	% Abundance
$^{11}B^+$	1.6×10^{-7}	7.17
$^{10}B^+$	4.0×10^{-8}	1.79
$^{104}Pd^{++}$	7.0×10^{-8}	3.13
$^{106}Pd^{++}$	5.0×10^{-8}	2.24
$^{105}Pd^{++}$	5.0×10^{-8}	2.24
$^{110}Pd^{++}$	2.0×10^{-8}	0.89
$^{104}Pd^+$	3.4×10^{-7}	15.24
$^{105}Pd^+$	4.8×10^{-7}	21.52
$^{106}Pd^+$	3.4×10^{-7}	15.24
$^{108}Pd^+$	3.2×10^{-7}	14.34
$^{110}Pd^+$	1.6×10^{-7}	7.17
$^{104}Pd^{11}B^+$	8.0×10^{-8}	3.58
$^{106}Pd^{11}B^+$	5.0×10^{-8}	2.24
$^{108}Pd^{11}B^+$	5.0×10^{-8}	2.24
$^{110}Pd^{11}B^+$	2.0×10^{-8}	0.89

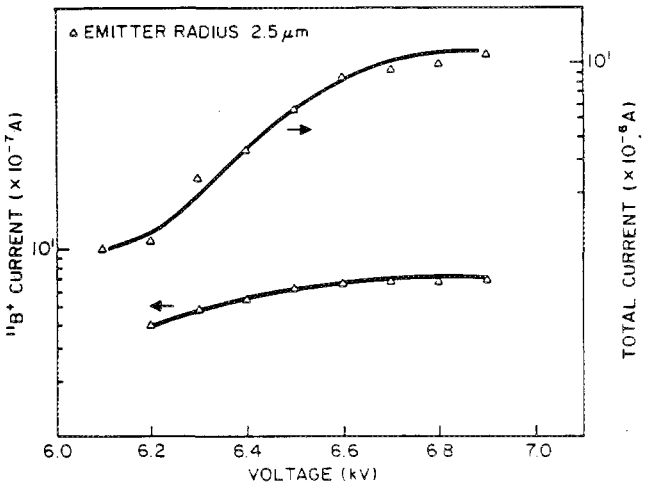

FIG. 3. $^{11}B^+$ and total current–voltage characteristics of 2.5-μm emitter tip radius.

ish the volume of the liquid at the tip. Therefore, steady-state flow rate can be achieved, and, consequently, beam fluctuation is small and emission becomes more stable. Figures 6(a)–6(c), show optical micrographs of the deposit obtained from a 2.5-μm emitter tip radius with no apparent droplet formation. Each particle has an approximate size of 0.5 μm, and the particulate distribution seems to follow beam Gaussian distribution pattern or bell shape distribution. The particle density is lower on the outside of the deposit [see Fig. 6(a)] and higher toward the center of the deposit [see Figs. 6(c) and 6(d)]. For larger emitter tip radius (10 μm), the flow rate is larger, therefore, Taylor cone[12] breakup is more likely to occur and produces larger beam fluctuation or unstable beam emission. Optical micrographs of the deposit on silicon substrate obtained from a 10-μm emitter tip show a "patchy" droplet formation on the surface of the silicon substrate [see Figs. 7(a)–7(d)]. The droplet distribution tends to be more intense toward the center [see

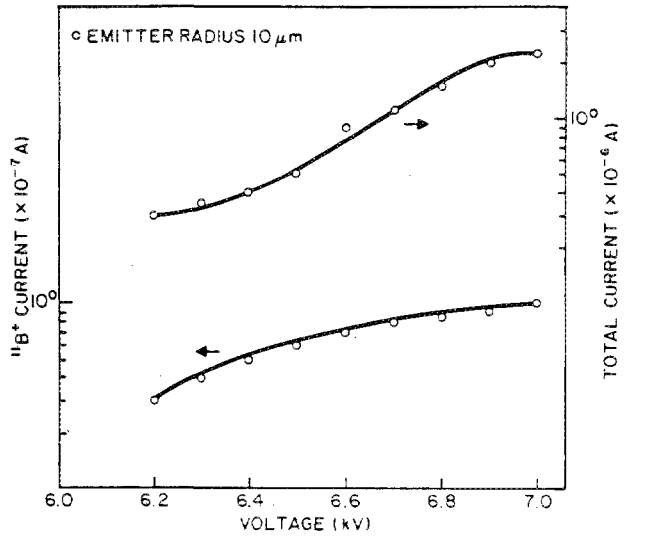

FIG. 4. $^{11}B^+$ and total current–voltage characteristics of 10-μm emitter tip radius.

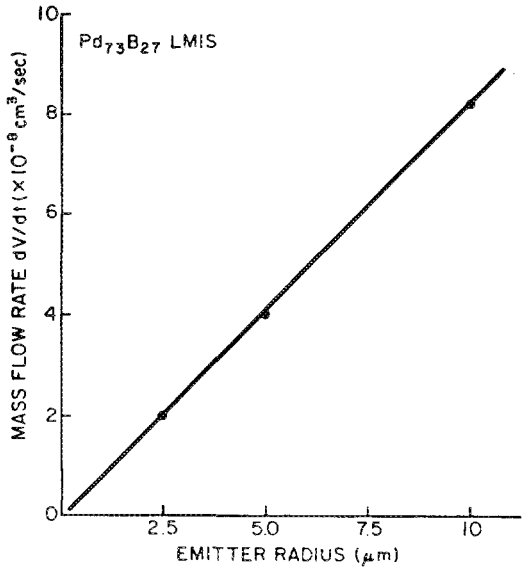

FIG. 5. Calculated plot of mass flow rate of palladium boride LMIS vs emitter tip radius.

Fig. 7(d)], and also tends to follow a Gaussian shape distribution pattern. Average size of the droplets varies from 5 to 30 μm.

Figure 8(a) shows as deposited Auger electron spectroscopy results of the deposit from a 10-μm emitter tip radius. Some of the elements such as Fe, Ni, Cr, and Re are the result of stainless-steel (Fe, Ni, Cr) extractor sputtering and emit-

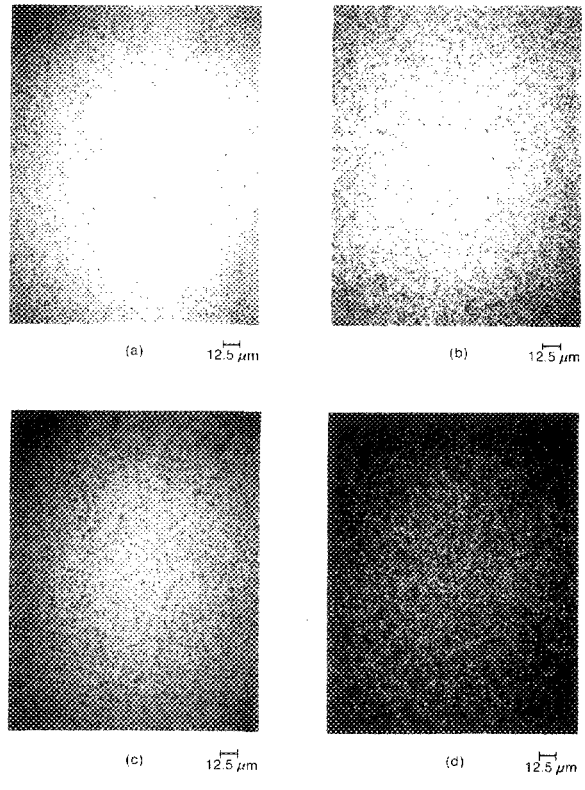

FIG. 6. Optical micrographs of LMIS deposition on silicon substrate obtained from 2.5-μm emitter tip radius. (a) Edge of deposit (b) and (c) near the center and (d) center.

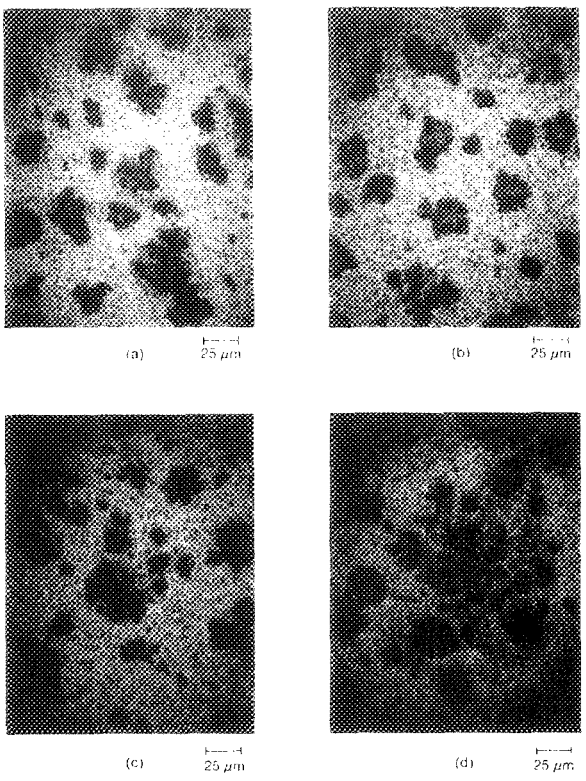

FIG. 7. Optical micrograph of LMIS deposition on silicon substrate obtained from 10-μm emitter tip radius. (a) Edge of deposit (b) and (c) near the center and (d) center.

ter tip erosion forming neutral ions and were not detected by QMS. The presence of boron species is not clearly evident in this spectrum. Figure 8(b) shows an Auger electron spectrum of the same sample after 3 min of argon ion milling. One can notice that the oxygen peak [present in Fig. 8(a)] disappears whereas the boron peak barely evident in Fig. 8(a) is shown more clearly.

Figure 9 shows Rutherford backscattering spectroscopy (RBS) results from a film of $Pd_{73}B_{27}$ deposited from 10-μm emitter tip on silicon substrate. The calculated stoichiometry ratio from RBS of the deposit resulting after 3-h deposition is $Pd_{76}B_{24}$, which remains as a eutectic composition, indicating that there is no significant change in composition between alloy source and the alloy deposited. This retention of composition is very desirable since the process produced no change in composition which is useful in microcoating for surface modification. However, other problems such as maintaining ion beam purity free from other contaminants, such as emitter erosion, remains a difficult task yet to be solved.

IV. CONCLUSIONS

Liquid metal ion sources have a potential application for direct writing of patterns such as conducting pathways in hybrid microcircuits as well as other applications, such as microcoating for surface modification. Smaller emitter radius (2.5 μm) produced uniform coating with no apparent droplet formation compared with larger emitter radius (10-μm tip). An interesting result obtained is that despite insta-

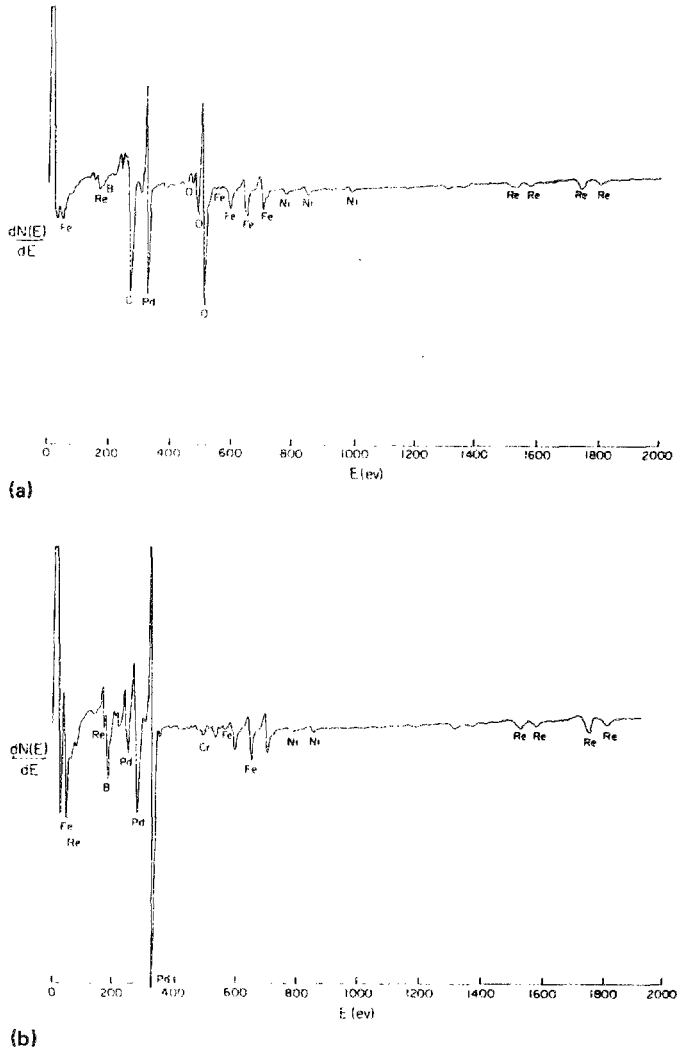

FIG. 8. Auger electron spectroscopy of LMIS deposit on silicon substrate. (a) As received (b) after 3-min argon ion milling.

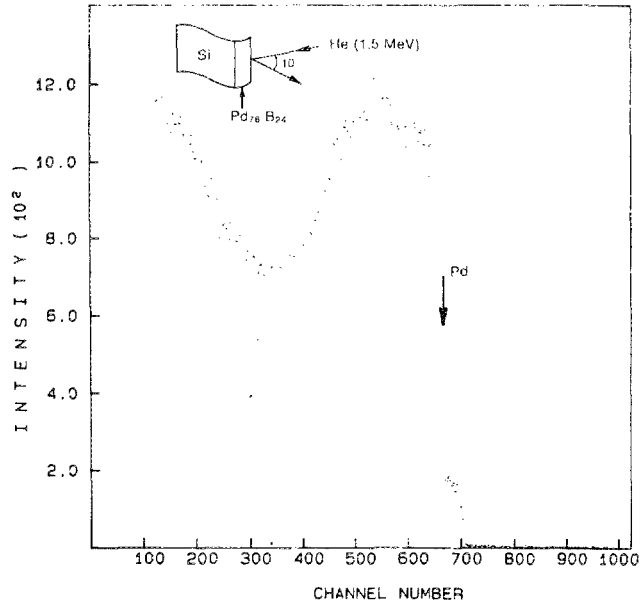

FIG. 9. Rutherford backscattering spectroscopy of LMIS deposit on silicon substrate.

bility associated with larger emitter tip (which produced more droplets on silicon substrate), the calculated stoichiometry resulting from RBS analysis shows no significant change in alloy composition and the eutectic characteristic is preserved between alloy source and the deposit even after 3 h of deposition. Auger electron spectroscopy shows that the main impurity of the alloy deposit comes from extractor sputtering due to location of emitter tip above extractor, and due to emitter tip erosion.

Future experiments will be conducted at shorter deposition times to verify the composition between alloy source and the deposit.

ACKNOWLEDGMENT

The authors gratefully acknowledge support of this work by the Semiconductor Research Corporation.

[1]R. Clampitt, K. L. Aitken, and D. K. Jefferies, J. Vac. Sci. Technol. **12**, 1208 (1975).
[2]R. L. Kubena, C. Anderson, R. L. Seliger, R. Julles, and E. Stevens, J. Vac. Sci. Technol. **19**, 916 (1981).
[3]K. Gamo, T. Ukegawa, Y. Inomoto, Y. Ochiai, and S. Namba, J. Vac. Sci. Technol. **19**, 1182 (1981).
[4]R. H. Higuchi-Rusli, Ph.D. thesis, Rensselaer Polytechnic Institute, 1986.
[5]F. G. Rudenauer, W. Steiger, E. Wiener, R. Grotzchel, and F. Nahring, Vacuum **35**, 315 (1985).
[6]A. Wagner, T. Venkatesan, P. M. Petroff, and D. Barr, J. Vac. Sci. Technol. **19**, 1186 (1981).
[7]C. Mahony and P. D. Prewett, Vacuum **34**, 301 (1984).
[8]T. Ishitani, A. Shimase, and H. Tamura, Appl. Phys. Lett. **39**, 627 (1981).
[9]P. D. Prewett, L. Gowland, K. L. Aitken, and C. Mahony, Thin Solid Films **80**, 117 (1981).
[10]R. H. Higuchi-Rusli, K. C. Cadien, J. C. Corelli, and A. J. Steckl, J. Vac. Sci. Technol. B **5**, 190 (1987).
[11]R. Gomer, Appl. Phys. **19**, 375 (1979).
[12]G. I. Taylor, Proc. R. Soc. London Ser. A **280**, 383 (1964).